Developmental Biology 537 (2026) 53–61

Contents lists available at ScienceDirect

Developmental Biology

journal homepage: www.elsevier.com/locate/developmentalbiology

Original research article

A parallel reporter assay for zebrafish

Gloria D. Ligunas [a,b], Stefan C. Materna [a,b,c,d,*]

[a] Department of Molecular and Cell Biology, University of California Merced, Merced, CA, 95343, USA
[b] Quantitative and Systems Biology Graduate Program, University of California Merced, Merced, CA, 95343, USA
[c] Health Sciences Research Institute, University of California Merced, Merced, CA, 95343, USA
[d] Center for Cellular and Biomolecular Machines, University of California Merced, Merced, CA, USA

ARTICLE INFO

Keywords:
Cis-Regulatory module
Gene regulation
Zebrafish
Tol2 transgenesis
Enhancer activity
Quantitative reporter analysis

ABSTRACT

Cis-regulatory modules (CRMs) are central to gene regulation, yet *in vivo* authentication of candidate CRMs remains a major bottleneck. Here, we introduce a parallel reporter assay for zebrafish that enables simultaneous, quantitative analysis of multiple transcriptional reporters using standard Tol2-mediated transgenesis. Activity of individual reporters is established through detection of a molecular barcode, allowing direct comparison of CRM activity within the same biological sample. We find that barcoded reporters function independently and that variability arising from mosaicism and genomic position effects is effectively mitigated by analyzing modest numbers of embryos routinely obtained in transient transgenesis experiments. Using whole embryos, we demonstrate robust detection of reporter activity across CRMs with distinct levels and spatial domains of activity. We further show that pre-enrichment enhances sensitivity. This enables cell type-specific comparisons of CRM activity and reveals context-dependent differences in amplitude. Together, these findings demonstrate that conventional zebrafish transgenesis supports reliable, multiplexed analysis of transcriptional reporters. This approach provides a practical framework for higher-throughput authentication of candidate CRMs *in vivo* and complements existing strategies for detailed spatial characterization.

1. Introduction

Gene regulatory sequence is organized into cis-regulatory modules (CRMs), pieces of non-coding DNA that control transcription of associated genes. CRMs integrate the regulatory information present in the nucleus and collectively drive the overall expression pattern of a gene. Aberrant regulation of gene expression can have profound consequences, from developmental defects to major human diseases, including cardiovascular disorders, diabetes, and cancer (Lee and Young, 2013; Wang et al., 2019). Accordingly, the vast majority of disease-associated sequence variants lies within non-coding regions with presumed regulatory function (Edwards et al., 2013; Ward and Kellis, 2012). The number of discrete CRMs associated with each gene correlates with the complexity of its expression pattern; from very few for genes with simple expression patterns to dozens for genes with highly dynamic expression patterns (Peter and Davidson, 2015; Singh et al., 2021). The number of discrete regulatory modules in the genome thus dwarfs the number of protein coding genes (Pennacchio et al., 2013; The ENCODE Project Consortium, 2012). Yet, due to technical challenges only a comparatively small number of CRM candidates has been tested experimentally.

CRMs are traditionally characterized in reporter assays, where a piece of DNA with suspected regulatory function is placed upstream of a detectable reporter (Alam and Cook, 1990; Chalfie et al., 1994). The reporter is then introduced into the system under study and reporter activity is evaluated. While reporter assays are easily performed in cell culture, cell lines are a poor proxy for the dynamic processes unfolding *in vivo,* particularly during embryogenesis. Establishing that CRMs recapitulate all or part of the overall expression pattern of associated genes requires reporter analysis in transgenic animals. Usually, CRMs are tested one at a time, a slow and labor-intensive undertaking even when working with transient transgenics.

Parallel reporter assays (PRAs) increase the throughput of traditional reporter assays. Although specific implementations differ, the general principle is to incorporate a unique sequence tag in the transcribed region of the reporter (Inoue and Ahituv, 2015; Kwasnieski et al., 2014; Ryan and Farley, 2020). By linking each reporter to its CRM, this barcode-based strategy permits parallel assessment of multiple reporters within the same assay. Established methods vary in barcode design, delivery, and detection. Most commonly, barcodes are unique artificial

* Corresponding author. Department of Molecular and Cell Biology, University of California Merced, Merced, CA, 95343, USA.
E-mail address: smaterna@ucmerced.edu (S.C. Materna).

https://doi.org/10.1016/j.ydbio.2026.06.007
Received 14 January 2026; Received in revised form 26 May 2026; Accepted 10 June 2026
Available online 13 June 2026

sequences; however, in some implementations, the CRM is placed downstream of the transcription start site and serves as its own barcode (Agarwal et al., 2025; Klein et al., 2020; Ryan and Farley, 2020). Delivery methods match the experimental system. Cultured cells can simply be transfected, whereas transgenic embryos are generated using model-specific methods, such as microinjection or electroporation. Detection methods include quantitative PCR (qPCR), RNA counting, and RNA-sequencing (Farley et al., 2015; Nam et al., 2010; Williams et al., 2019; Williams and Sauka-Spengler, 2021). The number of CRMs that can be tested simultaneously depends on the method of transgenesis, number of cells expressing the reporter, and the sensitivity of the detection method (Ryan and Farley, 2020).

Zebrafish are an excellent model for studying gene regulation. Embryos are readily available, transgenesis is routine, and reporter expression is easily assessed. Collectively, the zebrafish community has identified and used hundreds of different CRMs to label specific cell types and lineages. Despite this substantial achievement, the number of validated CRMs remains modest compared to the tens of thousands predicted across the zebrafish genome (Baranasic et al., 2022; Pennacchio et al., 2013). This disparity underscores the need for higher-throughput approaches to systematically identify and characterize CRMs in this model system.

Reporter analysis in zebrafish is facilitated by straightforward methods for introducing transgenes into the genome. These approaches vary in efficiency, copy number of integrated constructs, genomic location of insertion sites, and the extent of mosaicism. The most widely used system relies on the Tol2 transposase to achieve high rates of transgenesis. Tol2-based genomic integration results in many independent integration events per transgenic animal, and F_1 founder animals often contain multiple copies of a transgene (Kawakami, 2004; Kawakami et al., 2000). The high integration rate has been exploited to generate complex genetic mosaics by co-injecting barcoded reporters for clonal analysis and lineage tracing in F_0 animals (Wagner et al., 2018). This suggests that Tol2-mediated transgenesis can support simultaneous assessment of multiple reporters. Potential challenges include the comparatively high degree of mosaicism and position effects that arise from the near-random integration of reporter transgenes into the genome, both of which may reduce accuracy and increase noise.

Here, we introduce a parallel reporter assay for zebrafish that enables multiplexed, quantitative analysis of transcriptional regulation *in vivo*. Using Tol2-mediated transgenesis and barcode-based quantification, we simultaneously measure the activity of multiple transcriptional reporters within the same biological sample, enabling higher-throughput *in vivo* interrogation of CRM activity. We reasoned that the advantages of the Tol2 system—efficiency and independent genomic integration—outweigh its disadvantages, including position effects and mosaicism. We find that the impact of mosaicism and position effects can be mitigated, enabling reproducible measurement of regulatory amplitude in F_0 embryos. This framework allows direct comparison of CRM strength across elements and cell types, revealing context-dependent differences in transcriptional output that are difficult to assess in conventional, single-reporter assays.

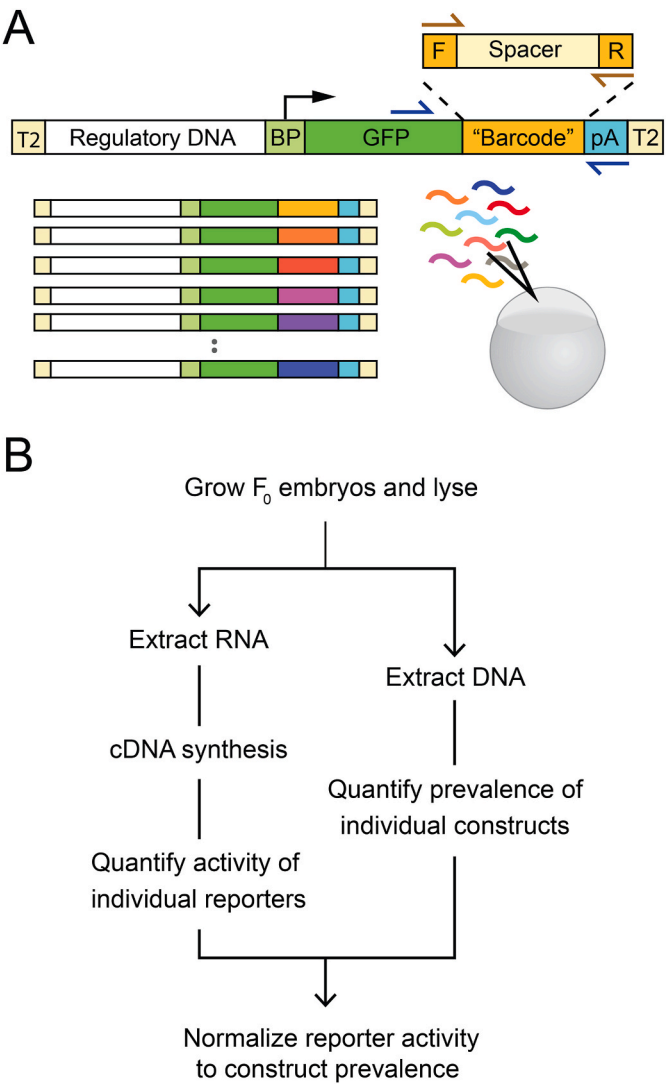

Fig. 1. Parallel reporter assay design and workflow. A) Schematic of barcoded reporter constructs. Candidate *cis*-regulatory modules (CRMs) are positioned upstream of a minimal basal promoter (BP) to drive GFP expression. The transcribed region includes unique barcode sequences that serve as primer binding sites for reporter-specific transcript quantification (orange arrows). Universal primer sites located in adjacent common regions enable pre-amplification of all reporters (blue arrows). The expression cassette is flanked by Tol2 transposase recognition sites (T2). Up to ten reporters are co-injected per experiment. pA, polyadenylation site. B) Workflow for parallel analysis of reporter activity. F_0 embryos are grown to the desired stage, after which DNA and total RNA are isolated from whole embryos or from sorted cells. Following cDNA synthesis, transcript abundance for individual reporters is quantified by PCR. Reporter levels are measured separately and used to normalize reporter activity.

2. Results

2.1. Assay design and workflow

To simultaneously test the activity of multiple reporters in zebrafish, we designed a parallel reporter assay that relies on Tol2-mediated transgenesis for integration into the genome and qPCR for reporter quantification. The design of the reporter system, depicted in Fig. 1A, is straightforward: the expression cassette is flanked by Tol2 recognition sites; CRM candidates are inserted upstream of a minimal promoter with low background activity derived from the *c-Fos* gene, which has been used in enhancer screens in zebrafish and optogenetic control systems (LaBelle et al., 2021; Scott, 2009). The basal promoter is followed by the GFP coding sequence, a unique identifier — the "barcode" — and the SV40 poly-adenylation sequence. The 20 bp at each end of the barcode are complementary to PCR primers used for quantification of individual reporters.

The general workflow of this assay, depicted in Fig. 1B, is as follows: barcoded reporter plasmids and *Tol2* mRNA are injected into the zygote using standard transgenesis (Suster et al., 2009). Embryos are grown to the relevant stage and lysed; total RNA and genomic DNA are then extracted separately. Following reverse transcription, activity of each individual reporter is quantified using qPCR with barcode-specific primers. F_0 embryos are mosaic and, to account for small differences in prevalence, we quantify each reporter in genomic DNA relative to a

single copy gene and use this to normalize reporter activity. As has been established in other systems, this step ensures that activities can be compared within and between assays (Nam et al., 2010). Finally, activity for each reporter is calculated relative to an inactive control that establishes background for the system.

2.2. Barcode design and test

To enable multiplexed reporter quantification, we established a panel of barcode-specific primer pairs with negligible cross-amplification under standard qPCR conditions. Candidate barcode/primer combinations were computationally screened and experimentally validated for specificity (see Materials and Methods). We selected ten reporter constructs for which off-target amplification was undetectable or comparable to background controls.

The dynamic range of reporter assays is determined by the ratio of active reporters over inactive controls, usually empty reporter plasmid. To establish baseline activity for our reporter system, and to ensure that background is homogenous, we co-injected all ten empty barcoded reporter plasmids into zygotes (*Tg(empty:GFP-BC1–10)*). We then measured activity of individual reporters relative to a commonly used housekeeping reference gene, *eef1a1l1* (McCurley and Callard, 2008).

Mean ΔC_t values for individual barcodes ranged from 13.4 to 15.1 cycles (n = 3), corresponding to an approximately 10,000-fold difference to *eef1a1l1*, indicating sufficient sensitivity to detect even weak reporter activity (Fig. 2A). ΔC_t values showed minimal variability within batches (SDs: 1.11, 0.59, and 0.75); differences in batch means reflected biological differences in *eef1a1l1* expression between embryo cohorts, which can be appreciable (Ligunas and Materna, 2026). Together, these data indicate that background signal from empty reporters is homogeneous, low, and reproducible.

While empty reporter constructs are commonly used as negative controls, they may exhibit low-level activation due to unintended enhancer trapping at the site of genomic integration. Such effects are difficult to predict and can complicate the interpretation of reporter background. As an alternative to empty reporters, we inserted the inactive *C120* CRM upstream of the basal promoter. *C120* is a short (120 bp) artificial sequence originally developed for optogenetic transcriptional control (Motta-Mena et al., 2014); it is specifically bound by the light-activated bacterial transcription factor EL222, which is absent from the zebrafish genome. In the absence of EL222, *C120* has been shown to exhibit negligible background activity (LaBelle et al., 2021). We injected all ten reporters, now containing the *C120* CRM (*Tg(C120:GFP-BC1–10)*), and measured reporter activity relative to *eef1a1l1*. Upon quantification, *C120*-containing reporters had background levels comparable to those of empty reporters (n = 3; Fig. 2B), with similar variability within batches (SDs = 1.15, 0.64, and 0.60).

Although quantitatively similar, we observed a qualitative difference between empty and *C120*-containing reporters. Embryos transgenic for empty reporters produced low background GFP expression—typically no more than a few cells, as is characteristic of Tol2-based transgenesis (Fig. 2C). In contrast, embryos carrying *C120* reporters consistently produced fewer GFP-positive cells (Fig. 2D). Reducing the number of GFP-positive cells in negative controls is advantageous for downstream applications such as fluorescence-activated cell sorting (FACS), where even sparse spurious GFP expression can affect enrichment. Accordingly, we used *C120*-containing reporters to establish baseline activity in all subsequent experiments.

2.3. Barcoded reporters are independent

Reporters must function independently, and CRM activity should not be affected by barcodes. To test this, we used the well-characterized *ubb* enhancer, which drives expression throughout the zebrafish embryo (Mosimann et al., 2011). Because *ubb* is expressed in all cells, mosaicism does not affect readout of *ubb* reporter activity as it might affect others with more restricted activity. By normalizing activity to the prevalence of each reporter, we are therefore able to directly compare activity levels between individual reporters.

We co-injected five "active" reporters, containing the *ubb* CRM, with five "inactive" reporters, containing only the *C120* CRM; we found that *ubb*-containing reporters (barcodes 1–5) are about 20-fold activated

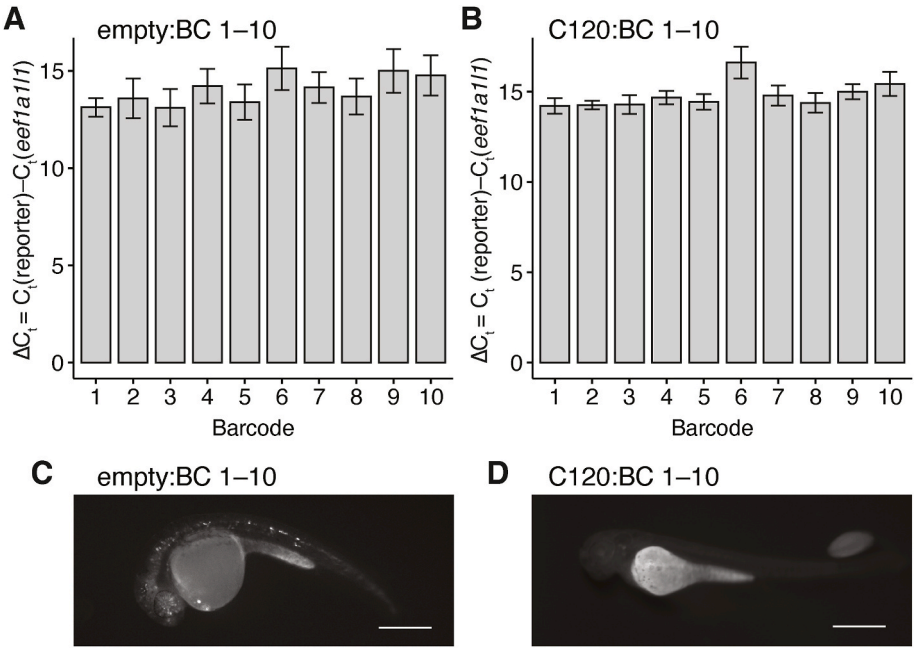

Fig. 2. Establishing baseline activity of barcoded reporters. A) Quantification of background activity of empty reporter constructs (*Tg(empty:GFP-BC1–10)*) at 24 hpf, measured relative to *eef1a1l1*. Bars represent mean $\Delta C_t \pm$ SD (n = 3). B) Quantification of background activity of *C120*-containing reporters at 24 hpf, relative to *eef1a1l1* reveals levels comparable to those of empty reporters. Bars represent mean $\Delta C_t \pm$ SD (n = 3). C) F_0 embryos injected with empty reporter show generally low background GFP expression at 24 hpf, typically confined to a few cells per embryo. Scale bar = 250 μm. D) F_0 embryos injected with *C120*-containing reporters (*Tg(C120:GFP-BC1–10)*) exhibit fewer GFP-positive cells throughout early development (representative embryo shown at 48 hpf).

($\Delta C_t = 4.36 \pm 0.86$ SEM, n = 3) over inactive *C120*-containing reporters (barcodes 6–10) (Fig. 3A). When we switched association of CRM and barcodes, reporters 6–10, now containing the "active" *ubb* CRM, were activated about 16-fold ($\Delta C_t = 3.98 \pm 0.69$ SEM, n = 3) over inactive controls (Fig. 3B). In each case, the difference between active and inactive reporters is statistically significant (Fig. 3C, left: $p = 1.4x10^{-7}$; right: $p = 9.5x10^{-9}$, Welch Two Sample *t*-test). We conclude that barcoded reporters function independently and, despite some variation, report consistent levels of CRM activity.

Tol2-mediated transgenesis generates numerous independent genomic integrations in F_0 embryos, resulting in mosaic reporter expression that is potentially sensitive to stochastic variation and position effects (Kawakami, 2004; Wagner et al., 2018). We therefore sought to establish sample collection conditions that would provide robust and reproducible measurements of reporter activity. Empirically, larger embryo pools produced more consistent measurements than smaller samples, consistent with averaging across many independent integration events. Pools of 100 embryos also readily yielded sufficient total RNA for downstream analysis. Using 5 μg of total RNA for cDNA synthesis consistently produced robust qPCR amplification with C_t values below 30, a range in which technical variability is reduced (Taylor et al., 2019). Based on these considerations, all subsequent experiments were performed using pools of 100 embryos and 5 μg total RNA for cDNA synthesis.

2.4. Whole-embryo analysis detects activity of lineage-restricted CRMs

We next tested if our assay enables simultaneous assessment of a diverse set of CRMs. In the zebrafish embryo cell fates diverge quickly, and, post-gastrulation, most cell types account for only a small fraction (Farrell et al., 2018; Sur et al., 2023; Wagner et al., 2018). Activity of CRMs associated with lineage restricted genes is similarly confined to small fractions, which our approach must be able to detect. We thus chose several well-characterized CRMs with a range of expression domains and activity levels and quantified their activity in whole embryos.

We included CRMs associated with the following four genes: *ubb*, *fli1*, *dll4*, and *myl7* and determined background with *C120*-containing reporter. The *ubb* CRM, already discussed above, drives ubiquitous expression in the embryo (Mosimann et al., 2011). Activity of the *fli* CRM, controlling transcription of the gene encoding the Fli1 transcription factor, is restricted to vascular endothelium (Lawson and Weinstein, 2002). Similarly, the *dll4in3* CRM is associated with the *delta-like 4* gene and is confined to arterial endothelium (Sacilotto et al., 2013). Last, the CRM controlling transcription of *myl7* (commonly referred to as *cmlc2*) is highly specific to cardiomyocytes (Huang et al., 2003). To assess reproducibility across independently barcoded reporters, we tested each CRM in two separate reporters.

We co-injected all ten barcoded reporters into zebrafish zygotes, collected embryos at 24 hpf, and quantified reporter activity (Fig. 4A). Of the four CRMs included, we found reporters containing three (*ubb*, *fli*, *cmlc2*) to be strongly activated; only *dll4in3* was indistinguishable from background (Fig. 4B). For each CRM/barcode pair, fold-activation values were similar between the two reporters, indicating that reporter activity is consistent across barcodes.

We co-injected all ten barcoded reporters into zebrafish zygotes and repeated the experiment across three independent biological replicate injections. Embryos were collected at 24 hpf and reporter activity was quantified from whole-embryo lysates. Of the four CRMs included, we found reporters containing three (*ubb*, *fli*, *cmlc2*) to be strongly activated. Only *dll4in3* was indistinguishable from background. For each CRM, values obtained from the two independent barcode reporters were highly similar across biological replicates and were therefore combined for downstream analysis of CRM activity.

ubb-containing reporters were activated 76-fold, a large and statistically robust difference (ΔC_t(*ubb–C120*) $= 6.25 \pm 1.15$ SEM; $p = 1.4x10^{-5}$, Dunnett's test) (Fig. 4). Reporters containing the *fli* CRM were activated 11-fold ($\Delta C_t = 3.47 \pm 1.37$ SEM, $p = 0.012$, Dunnett's test), and *cmlc2* CRMs were activated 8-fold activation over controls (ΔC_t: 3 ± 0.94, $p = 0.032$ SEM, Dunnett's test). The comparatively lower activity of *fli* and *cmlc2* CRMs, on a per-embryo basis, is expected because they are active in only a small fraction of cells in the embryo. At 24 hpf, vascular endothelial cells comprise only about 2% of the embryo (Gurung et al., 2022), while cardiomyocytes account for roughly 0.3% (De Pater et al., 2009). When cell type prevalence is considered to estimate activity per cell, *cmlc2* is the strongest driver of transcription, followed by *fli*. This is consistent with the widespread use of the *cmlc2* CRM for strong cardiomyocyte-specific transgene expression. In contrast, *dll4in3* activity may be too weak to be detected in whole-embryo lysates at this stage. Nonetheless, our parallel reporter system reliably detects transcriptional activity of validated CRMs using total RNA from whole embryo lysates.

2.5. Enrichment of reporter-positive cells improves sensitivity

Cells lacking reporter activity add to background without contributing meaningful signal. We therefore hypothesized that enriching for reporter-positive cells within the relevant cell type would increase sensitivity.

Three of the four CRMs included above drive transcription in vascular endothelium (*fli*, *dll4in3*, *ubb*); we thus tested reporter activity specifically in this cell type. We injected the same ten barcoded reporters as above into *Tg(flk-1:ras-mCherry)* zygotes and repeated the experiment across four independent biological replicate injections; each CRM was represented by two independently barcoded reporters. Embryos were grown until 24 hpf. Following dissociation, we obtained reporter-positive endothelial cells by FACS, gating first for vascular endothelium (mCherry), then reporter (GFP) (Fig. 5A). For reliable quantification we aimed at recovering approximately 5000 cells. Starting with 300 injected embryos, we were able to consistently collect between 4500 and 5000 double-positive ($mCherry^+$;GFP^+) cells (4728 ± 383). To ensure robust detection, we performed 10 rounds of pre-amplification using universal primers (Fig. 1) prior to reporter quantification with barcode-specific primers, as described above. Reporter activity measurements obtained from the two barcode reporters were highly similar across biological replicates and were therefore combined for downstream analysis of CRM activity.

As in whole embryos, *ubb*-containing reporters were significantly activated above background in endothelial cells; however, the magnitude of activation was lower (~10-fold; $\Delta C_t = 3.3 \pm 1.46$ SEM, $p = 0.017$, Dunn's test) than in whole embryos (~76-fold) (Fig. 5B). In contrast, *fli*-containing reporters were about 63-fold activated ($\Delta C_t = 5.97 \pm 1.37$ SEM, $p = 0.35 \times 10^{-5}$,Dunn's test). This represents an approximately 6-fold increase in activation relative to whole embryos (~11-fold), which was statistically significant. *dll4in3*-containing reporters were activated 2.5-fold over background ($\Delta C_t = 1.32 \pm 0.74$ SEM, $p = 0.08$, Dunn's test). *dll4in3* reporter activity was elevated above baseline but did not reach statistical significance. Last, the *cmlc2* CRM is specific to cardiomyocytes and not active in vascular endothelium. Nonetheless, *cmlc2* reporter activity was somewhat elevated over background (2.6-fold, $\Delta C_t = 1.39 \pm 0.92$ SEM, $p = 0.073$, Dunn's test) although significantly less so than in whole embryo samples. Like *dll4in3*, *cmlc2* reporter activity was not statistically significant. The residual signal from *cmlc2* reporters may be true signal from cardiomyocytes accidently included in our sample or from ectopic expression in endothelium. This notwithstanding, the observed increase in *fli* and *dll4in3* signal, as well as the reduced *cmlc2* activity, suggests that using sorted endothelial cells provides a more accurate estimate of CRM activity in this cell type.

The *ubb* CRM is active in all cells of the embryo, which enables us to directly compare activity levels between whole embryos and sorted cells. As discussed above, *ubb* reporter was 76-fold activated over background in whole embryos but only 10-fold in endothelial cells, a

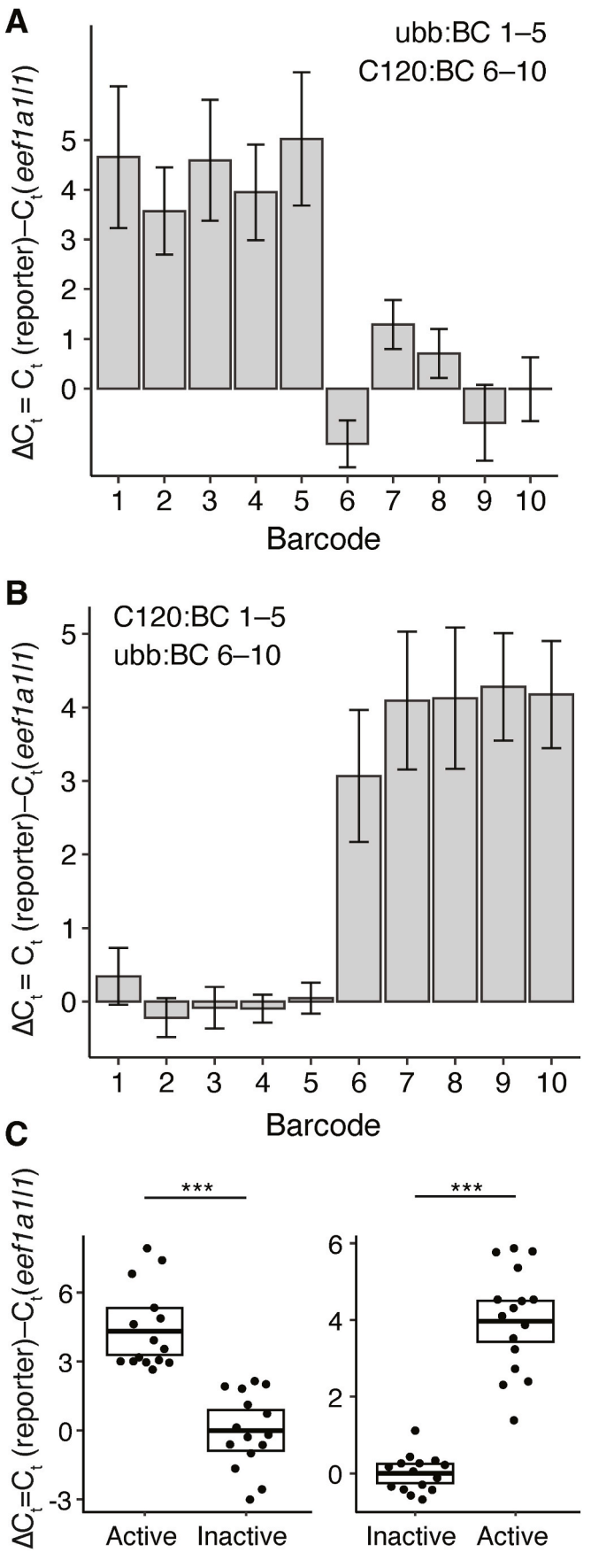

(caption on next column)

Fig. 3. Barcoded reporters function independently of barcode identity. (A) Co-injection of five reporters containing an active CRM (*ubb:GFP-BC1–5*) together with five reporters containing an inactive control element (*C120:GFP-BC6–10*). Quantification shows that *ubb*-containing reporters are consistently activated relative to *C120*-containing controls. Bars represent mean ± SEM (n = 3). B) Inverse barcode assignment, pairing inactive *C120* with BC1–5 and *ubb* with BC6–10. C) Combined summary of both experiments showing individual data points for all reporters. Differences between *ubb*-containing and *C120*-containing reporters are highly significant and independent of barcode association ($p < 0.001$). Center line indicates the mean; box denotes SEM.

large and significant difference (Welch's *t*-test, t(11.9) = 2.24, p = 0.045). This suggests that the *ubb* CRM is a weaker driver of transcription in endothelial cells compared to the embryo as a whole.

3. Discussion

In many animal models, including zebrafish, analysis of candidate CRMs relies on inherently low-throughput approaches. Here we established a reporter system for zebrafish that enables multiplexed quantitative analysis using standard transgenesis techniques. Using well-characterized CRMs, we demonstrate robust quantification of reporter activity spanning two orders of magnitude. This dynamic range is comparable to that observed in cell-culture-based reporter assays and can be achieved using embryo numbers typical of standard transgenesis experiments. Comparisons to highly abundant endogenous transcripts suggest that substantially larger signal differences can likely be resolved, indicating that the assay is capable of capturing a broad range of CRM activity. Mosaicism and position effects, common side effects of Tol2-based transgenesis, are mitigated by averaging across the large number of independent genomic integrations commonly obtained in F_0 animals.

Parallel reporter systems have been used in zebrafish to comprehensively query post-transcriptional regulation, where RNA-based reporters are delivered into the zygote in large numbers (Rabani et al., 2017; Reimão-Pinto et al., 2025). In contrast to DNA-based transcriptional reporters, these assays do not require integration into the genome, thus avoiding mosaicism and position effects.

The inherent mosaicism of Tol2 mediated transgenesis has been exploited for lineage analyses in multiplexed reporter assays (Wagner et al., 2018); here, ubiquitously active transcriptional reporters were barcoded with a unique molecular identifier and introduced into the zebrafish genome. Analysis by single cell RNA-sequencing revealed many, often nested clones, whose relationship enabled inference of lineage relationships (Wagner et al., 2018). These studies established strategies for parallel reporter analysis in zebrafish but avoided, or even exploited, mosaicism. By contrast, the central question motivating our study was whether mosaicism itself would prevent reliable quantification of reporter activity.

In standard Tol2-based transgenesis, most integration events occur not at the 1-cell stage but during early cleavage, resulting in mosaicism. However, when integration occurs, multiple reporter copies are often inserted independently into the genome of the same cell, a pattern reflected in the copy numbers inherited by F_1 founders (Kawakami, 2004). Although the earliest integrations generate the largest clones, many additional integrations, often dozens, occur in smaller clones (Wagner et al., 2018). Together, these smaller clones contribute substantially to overall reporter expression, thereby reducing variability arising from mosaicism and genomic position effects. While integrations occurring within the same genomic region could in principle produce correlated effects on reporter activity, averaging across many independent integration events and embryos is expected to minimize such biases. Consequently, sufficiently large samples effectively average across many independent integrations, such that local effects of individual insertion sites or clustered integrations are expected to contribute primarily stochastic noise rather than systematic bias.

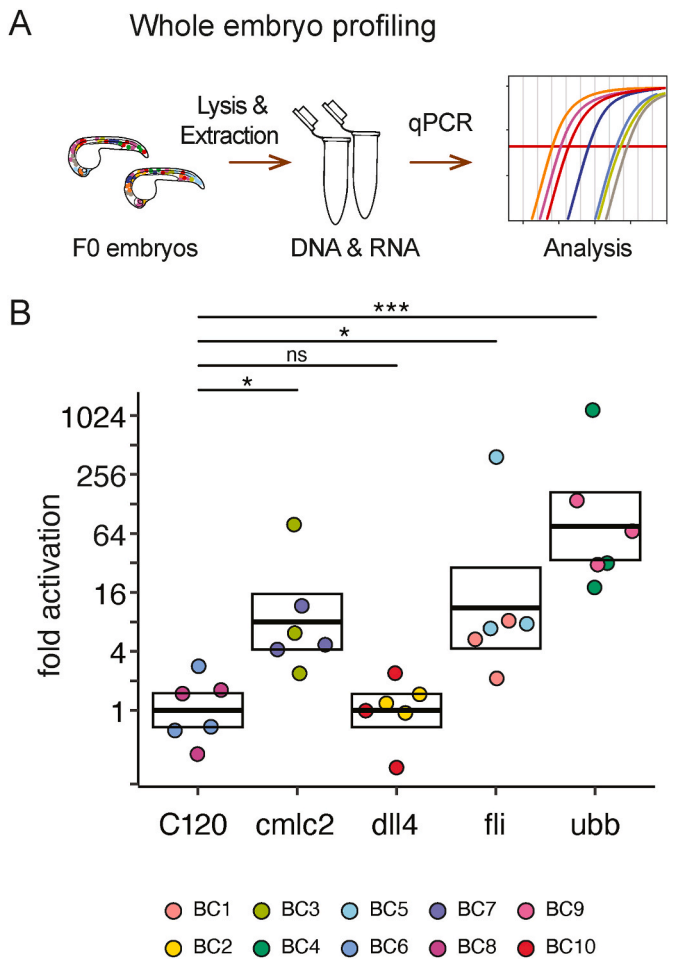

Fig. 4. Parallel reporter assays detect CRM activity in whole embryos. Activity of barcoded reporters containing the *cmlc2*, *dll4i3*, *fli*, and *ubb* CRMs was quantified in whole embryos relative to the inactive control (*C120*). Reporters containing the ubiquitous *ubb* CRM produced the strongest signal, whereas *dll4in3* reporter activity did not exceed background. Each CRM was tested using two independent barcoded reporters across three biological replicate experiments. Barcodes are color-coded as indicated. Individual points represent barcode-specific measurements from independent biological replicates. The center line represents the mean and the box denotes the SEM. $*p < 0.05$; $***p < 0.001$; n.s., not significant.

Using one-hundred whole embryos, we detected significant activity for three well-studied CRMs, *cmlc2*, *fli*, and *ubb,* without pre-enrichment or pre-amplification. Although signal was highest for *ubb,* which is active throughout the embryo, *fli* and *cmlc2* drove robust transcription, despite being restricted to comparatively small cellular fractions of the embryo; both are stronger drivers on a per-cell basis than *ubb*, consistent with qualitative assessment of fluorescent intensity. Thus, although whole-embryo analysis cannot distinguish between "low and ubiquitous" and "restricted but highly active" CRMs, this approach is well suited for authentication and comparative analysis of candidate CRMs.

Regulatory activity is highly context-dependent and distributed across diverse cell types. To capture cell type-specific information, we determined reporter activity in vascular endothelial cells. By quantifying multiple reporters in the same sample, we were able to directly compare their amplitude in this cell type. Our measurements confirm the above conclusion, drawn from whole embryo experiments, that *fli* is a stronger driver of transcription than *ubb*. Furthermore, our data suggest that *ubb* activity is weaker in vascular endothelial cells than across the embryo as a whole, indicating that the amplitude of this CRM, and likely others with ubiquitous activity, is context dependent.

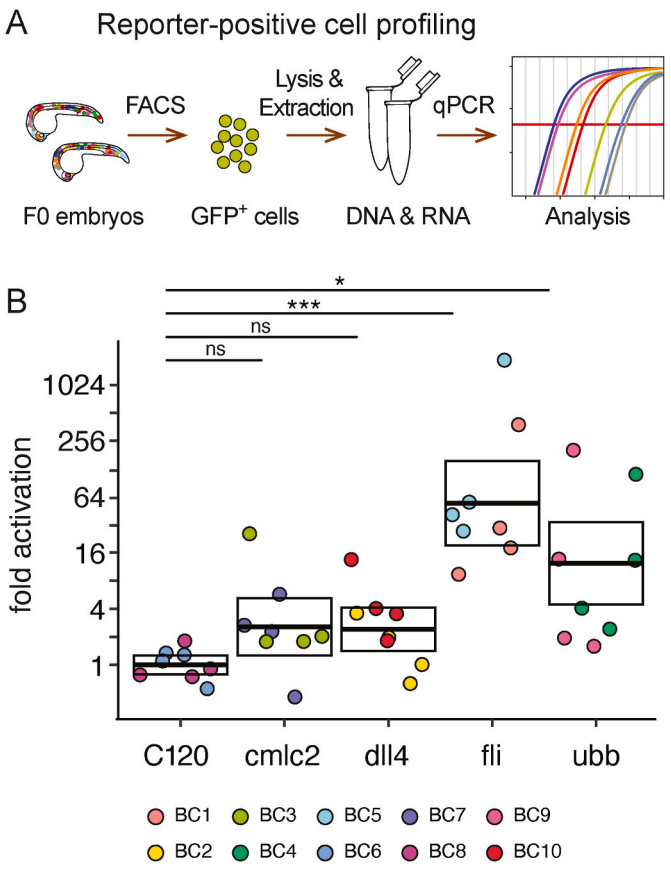

Fig. 5. Parallel reporter analysis reveals cell-type–specific CRM activity in sorted vascular endothelial cells. Activity of barcoded reporters was quantified in sorted vascular endothelial cells relative to the inactive control (*C120*). Reporters containing the *fli* CRM showed the strongest activation in this cell type. *ubb*-containing reporters were significantly activated over controls, but to a lesser extent than in whole embryos. *dll4in3* reporter activity was elevated relative to baseline, although the difference from *C120* was not statistically significant. Each CRM was tested using two independent barcoded reporters across four biological replicate experiments. Individual points represent barcode-specific measurements from independent biological replicates. Barcodes are color-coded as indicated. The center line represents the mean, and the box denotes the SEM. $*p < 0.05$; $***p < 0.001$; n.s., not significant.

Whole-embryo measurements and spatially resolved approaches represent complementary strategies with distinct tradeoffs between throughput, sensitivity, and cellular resolution. Candidate CRMs identified in whole-embryo screens can subsequently be evaluated in specific cell types using pre-enrichment or orthogonal approaches such as imaging or single-cell transcriptomics to achieve improved spatial resolution. Enrichment-based strategies therefore provide a practical intermediate approach between whole-embryo measurements and fully spatially resolved methods. Continued development of lineage- and cell-state-specific reporter lines should further enable reporter quantification within increasingly refined cellular populations.

Biological variability and minor staging differences likely contribute to the comparatively large variability in our measurements. In addition, qPCR is inherently noisy at low template abundance, which limits sensitivity (Taylor et al., 2019). This prevents statistical significance for activity of *dll4in3*-containing reporters; *dll4in3* CRM is a comparatively weak driver of transcription prior to the onset of blood flow (Sacilotto et al., 2013). *dll4* transcript levels rise steeply once circulation starts and peak near 30 hpf (Ligunas and Materna, 2026), placing our sampling window within a period of rapid change. Accordingly, *dll4in3* reporter measurements are likely highly sensitive to small staging differences, highlighting developmental timing as an important practical

consideration for quantitative reporter assays in developmental systems.

Quantification by qPCR currently represents the principal limitation for scaling the assay. For weak CRMs, reporter activity approaches the lower detection boundary, while increasing the number of barcodes requires additional primer pairs that must avoid cross-amplification and primer-interference effects in highly multiplexed reactions. We chose a relatively conservative barcode number in the present study to prioritize robustness and reproducibility. Nevertheless, our results demonstrate that standard Tol2-based transgenesis is well suited for simultaneous quantitative assessment of multiple reporters in zebrafish and should be adaptable to substantially larger reporter sets, potentially encompassing dozens of candidate CRMs.

Potential future uses include systematic *in vivo* validation of candidate CRMs emerging from genome-wide discovery pipelines, comparative analysis of enhancer variants, and functional dissection of regulatory elements through mutagenesis or serial deletion analysis. Sequencing-based quantification strategies may further improve scalability and sensitivity by reducing constraints associated with multiplexed primer design while increasing dynamic range and throughput.

Genome-wide discovery pipelines based on chromatin accessibility or transcription factor occupancy routinely produce extensive lists of candidate CRMs, yet these are rarely authenticated *in vivo* at scale. A complete understanding of gene regulation, however, requires not only identification of regulatory elements, but also characterization of their spatial activity, timing, and transcriptional amplitude. While spatial domains can increasingly be inferred from sequence features (Avsec et al., 2021; Singh et al., 2021; Wan et al., 2026), the quantitative strength of a CRM is not directly predictable from profiling data and must instead be measured.

Parallel reporter assays directly address this gap by enabling many CRMs, enhancer variants, or systematically mutated derivatives to be evaluated simultaneously within the same experimental context. This multiplexed framework enables quantitative comparisons that would otherwise be impractical at scale. In future implementations, integration with imaging-based quantification or single-cell transcriptomic approaches may further improve spatial and cell-type-specific resolution in complex samples. Although such strategies will likely involve tradeoffs between throughput, sensitivity, and experimental complexity, they provide a path toward increasingly comprehensive *in vivo* characterization of CRM activity.

These assays complement emerging workflows for creating stable transgenic lines. For instance, the piglet safe-harbor approach is a valuable recent addition to the zebrafish toolkit eliminating position effects and enables highly reproducible characterization of transcriptional reporters (Lalonde et al., 2024). However, each stable line evaluates only a single construct, limiting throughput. In contrast, multiplexed PRAs sacrifice precise control over integration site in exchange for the ability to compare many candidate regulatory elements simultaneously within the same experimental context. A productive strategy may therefore combine both approaches—using PRAs for broad discovery and comparative screening, followed by detailed spatial characterization of selected reporters using stable transgenic systems.

While the present study focuses on Tol2-mediated transgenesis in zebrafish embryos, the general strategy should be adaptable to additional transposon systems and model organisms. Our approach therefore provides a quantitative foundation for future higher-throughput platforms aimed at large-scale CRM discovery, enhancer dissection, and functional analysis of regulatory variants in zebrafish.

4. Materials and method

4.1. Zebrafish

Adult *Danio rerio* zebrafish were maintained under standard laboratory conditions (Westerfield, 2007). Our zebrafish wild type fish are outbred in a combined AB/TL/EKW background. For sorting vascular endothelial cells, we used the previously described *Tg(flk1:ras-Cherry)*^{S896} line (Chi et al., 2008). Experiments were performed in accordance with an approved IACUC protocol (UC Merced, protocol #2023-1144).

4.2. Generation of barcoded vectors

Barcode sequences were designed as unique 20mers serving as qPCR primer binding sites for barcode-specific amplification, separated by a common linker sequence (Nam et al., 2010). Sequences were designed for a predicted melting temperature of 60°C. Candidate barcode and primer sequences were computationally screened to minimize similarity to the zebrafish genome (GRCz11), cross-hybridization with other barcode sequences, and primer-primer interactions (Untergasser et al., 2012). Primer specificity was provisionally evaluated by PCR on zebrafish genomic DNA to identify primer pairs prone to nonspecific amplification. Barcodes were synthesized and inserted into pμTol2 backbone, linearized with *XbaI* using enzymatic assembly (Gibson et al., 2009; LaBelle et al., 2021). Following assembly of reporter constructs, barcode-specific primer pairs were further tested using pooled barcoded reporter plasmids supplemented with zebrafish genomic DNA, while omitting the corresponding target construct from the reaction. Primer sets showing evidence of cross-amplification were excluded. Ten barcode/primer combinations with negligible off-target amplification were selected for subsequent experiments.

Sequences of all barcodes and qPCR primers are provided in Supplemental Table 1. CRMs (*dll4in3* (Sacilotto et al., 2013); *fli1a* (Lawson and Weinstein, 2002); *myl7* (Huang et al., 2003); *ubb* (Mosimann et al., 2011) and the *5xC120* light-response element (Motta-Mena et al., 2014) were inserted upstream of the c-Fos basal promoter (Scott, 2009) of pμTol2-BC to obtain the following plasmids: pμTol2-dll4i3_cFos:GFP-BC; pμTol2-fli1a_cFos:GFP-BC; pμTol2-myl7_cFos:GFP-BC; pμTol2-5XC120_cFos:GFP-BC; and pμTol2-ubb:GFP-BC. Correct assembly was confirmed by sequencing.

4.3. Transgenesis

For Tol2-mediated transgenesis, a mix of barcoded reporter plasmids and Tol2 mRNA were co-injected into zygotes according to standard protocols (Suster et al., 2009). Embryos were grown under standard laboratory conditions (28.5°C) until the desired time, and, after ensuring proper staging (Kimmel et al., 1995), harvested.

4.4. DNA/RNA extraction

DNA/RNA extraction was performed using the Qiagen AllPrep DNA/RNA micro kit according to manufacturer's instructions with the following modifications: Up to 50 embryos were lysed in 500 μl of Buffer RLT Plus. If more than 50 embryos were lysed, the sample was split in two; nucleic acid extraction was performed separately, but samples were combined following elution. For on-column DNA removal during RNA extraction, we doubled the DNAse concentration and extended incubation to 1 h at room temperature. Both RNA and DNA was eluted by adding 100 μl of preheated nuclease free water, followed by a 10 min incubation at 60°C prior to centrifugation. After elution RNA and DNA was ethanol precipitated and resuspended in 10 μl nuclease-free water. Linear polyacrylamide was added to sorted samples to aid in precipitation.

4.5. Reverse transcription

2–10 μg of total RNA was reverse transcribed using Thermo Maxima H RT Master Mix Solution according to manufacturer's instructions. Following reverse transcription, the volume was adjusted to 50 μl.

4.6. Pre-amplification

cDNA was pre-amplified using the Promega GoTaq PCR Mix with the following program: 98°C–2 min, 10x(98°C–5 s, 60°C–15 s, 72°C–30 s), 72°C–10 min. The PCR reaction was column purified using the IBI PCR Clean Up kit and eluted in 50 µl. Reporter activity was quantified as described above. Universal primers used for preamplification were Fwd: 5′-ACGACGGCAACTACAAGACC-3′; Rev: 5′-CACTGCATTC-TAGTTGTGGTTTGTCC-3′.

4.7. Quantification of reporter expression

Activity of individual reporters was quantified by qPCR using 1 µl of the above cDNA solution per reaction; reactions were performed in triplicate and C_t values were averaged. Reporter activity was calculated relative to inactive controls. Background activity was established relative to *eef1a1l1* (Ligunas and Materna, 2026). We quantified reporter constructs in genomic DNA relative to the single-copy gene *prox1a* (all primer sequences are listed in Supplemental Table 1). We tested primer efficiencies by serial dilution to ensure amplification efficiency was between 1.95 and 2 (Wong and Medrano, 2005). To account for small differences in prevalence, reporter activity was normalized to plasmid abundance (Nam et al., 2010). Statistical analysis was performed using R. We tested whether our data was normally distributed using the Shapiro-Wilk test. For multiple comparisons, Kruskal-Wallis rank sum tests were used followed by Dunn's *post hoc*, unless noted; alpha was set to 0.05.

4.8. Embryo dissociation and sorting

To prepare samples for sorting, barcoded reporter injected *Tg(flk:ras-mCherry)*^{S896} (Chi et al., 2008) embryos were dechorionated at 24 hpf by mechanical agitation in 0.5 mg/ml pronase (Sigma-Aldrich) in 0.3x Ringer's solution. Deyolking and dissociation was performed as described previously (Manoli and Driever, 2012). Cells were sorted straight into RLT Plus lysis buffer using an Aria III cell sorter (BD Biosciences).

CRediT authorship contribution statement

Gloria D. Ligunas: Conceptualization, Data curation, Formal analysis, Investigation, Methodology, Software, Validation, Visualization, Writing – review & editing. **Stefan C. Materna:** Conceptualization, Data curation, Formal analysis, Funding acquisition, Investigation, Methodology, Project administration, Resources, Supervision, Validation, Visualization, Writing – original draft, Writing – review & editing.

Conflict of interest statement

The authors declare that they have no known competing financial interests or personal relationships that could have appeared to influence the work reported in this paper.

Acknowledgements

We thank the UC Merced vivarium team for animal care, and Dr. Gravano for help with cell sorting. We would like to thank the members of the Woo and Materna labs for many insightful discussions and suggestions.

Appendix A. Supplementary data

Supplementary data to this article can be found online at https://doi.org/10.1016/j.ydbio.2026.06.007.

Data availability

Data will be made available on request.

References

Agarwal, V., Inoue, F., Schubach, M., Penzar, D., Martin, B.K., Dash, P.M., Keukeleire, P., Zhang, Z., Sohota, A., Zhao, J., Georgakopoulos-Soares, I., Noble, W.S., Yardımcı, G. G., Kulakovskiy, I.V., Kircher, M., Shendure, J., Ahituv, N., 2025. Massively parallel characterization of transcriptional regulatory elements. Nature 639, 411–420. https://doi.org/10.1038/s41586-024-08430-9.

Alam, J., Cook, J.L., 1990. Reporter genes: application to the study of mammalian gene transcription. Anal. Biochem. 188, 245–254. https://doi.org/10.1016/0003-2697(90)90601-5.

Avsec, Ž., Agarwal, V., Visentin, D., Ledsam, J.R., Grabska-Barwinska, A., et al., 2021. Effective gene expression prediction from sequence by integrating long-range interactions. Nat. Methods 18 (10), 1196–1203. https://doi.org/10.1038/s41592-021-01252-x.

Baranasic, D., Hörtenhuber, M., Balwierz, P.J., Zehnder, T., Mukarram, A.K., Nepal, C., Várnai, C., Hadzhiev, Y., Jimenez-Gonzalez, A., Li, N., Wragg, J., D'Orazio, F.M., Relic, D., Pachkov, M., Díaz, N., Hernández-Rodríguez, B., Chen, Z., Stoiber, M., Dong, M., Stevens, I., Ross, S.E., Eagle, A., Martin, R., Obasaju, O., Rastegar, S., McGarvey, A.C., Kopp, W., Chambers, E., Wang, D., Kim, H.R., Acemel, R.D., Naranjo, S., Łapiński, M., Chong, V., Mathavan, S., Peers, B., Sauka-Spengler, T., Vingron, M., Carninci, P., Ohler, U., Lacadie, S.A., Burgess, S.M., Winata, C., Van Eeden, F., Vaquerizas, J.M., Gómez-Skarmeta, J.L., Onichtchouk, D., Brown, B.J., Bogdanovic, O., Van Nimwegen, E., Westerfield, M., Wardle, F.C., Daub, C.O., Lenhard, B., Müller, F., 2022. Multiomic atlas with functional stratification and developmental dynamics of zebrafish cis-regulatory elements. Nat. Genet. 54, 1037–1050. https://doi.org/10.1038/s41588-022-01089-w.

Chalfie, M., Tu, Y., Euskirchen, G., Ward, W.W., Prasher, D.C., 1994. Green fluorescent protein as a marker for gene expression. Science 263, 802–805. https://doi.org/10.1126/science.8303295.

Chi, N.C., Shaw, R.M., Jungblut, B., Huisken, J., Ferrer, T., Arnaout, R., Scott, I., Beis, D., Xiao, T., Baier, H., Jan, L.Y., Tristani-Firouzi, M., Stainier, D.Y.R., 2008. Genetic and physiologic dissection of the vertebrate cardiac conduction system. PLoS Biol. 6, e109. https://doi.org/10.1371/journal.pbio.0060109.

De Pater, E., Clijsters, L., Marques, S.R., Lin, Y.-F., Garavito-Aguilar, Z.V., Yelon, D., Bakkers, J., 2009. Distinct phases of cardiomyocyte differentiation regulate growth of the zebrafish heart. Development 136, 1633–1641. https://doi.org/10.1242/dev.030924.

Edwards, S.L., Beesley, J., French, J.D., Dunning, A.M., 2013. Beyond GWASs: illuminating the dark road from association to function. Am. J. Hum. Genet. 93, 779–797. https://doi.org/10.1016/j.ajhg.2013.10.012.

Farley, E.K., Olson, K.M., Zhang, W., Brandt, A.J., Rokhsar, D.S., Levine, M.S., 2015. Suboptimization of developmental enhancers. Science 350, 325–328. https://doi.org/10.1126/science.aac6948.

Farrell, J.A., Wang, Y., Riesenfeld, S.J., Shekhar, K., Regev, A., Schier, A.F., 2018. Single-cell reconstruction of developmental trajectories during zebrafish embryogenesis. Science 360, eaar3131. https://doi.org/10.1126/science.aar3131.

Gibson, D.G., Young, L., Chuang, R.-Y., Venter, J.C., Hutchison, C.A., Smith, H.O., 2009. Enzymatic assembly of DNA molecules up to several hundred kilobases. Nat. Methods 6, 343–345. https://doi.org/10.1038/nmeth.1318.

Gurung, S., Restrepo, N.K., Chestnut, B., Klimkaite, L., Sumanas, S., 2022. Single-cell transcriptomic analysis of vascular endothelial cells in zebrafish embryos. Sci. Rep. 12, 13065. https://doi.org/10.1038/s41598-022-17127-w.

Huang, C., Tu, C., Hsiao, C., Hsieh, F., Tsai, H., 2003. Germ-line transmission of a myocardium-specific GFP transgene reveals critical regulatory elements in the cardiac myosin light chain 2 promoter of zebrafish. Dev. Dyn. 228, 30–40. https://doi.org/10.1002/dvdy.10356.

Inoue, F., Ahituv, N., 2015. Decoding enhancers using massively parallel reporter assays. Genomics 106, 159–164. https://doi.org/10.1016/j.ygeno.2015.06.005.

Kawakami, K., 2004. Transgenesis and gene trap methods in zebrafish by using the Tol2 transposable element. In: Methods in Cell Biology. Elsevier, pp. 201–222. https://doi.org/10.1016/S0091-679X(04)77011-9.

Kawakami, K., Shima, A., Kawakami, N., 2000. Identification of a functional transposase of the *Tol2* element, an *Ac* -like element from the Japanese medaka fish, and its transposition in the zebrafish germ lineage. Proc. Natl. Acad. Sci. 97, 11403–11408. https://doi.org/10.1073/pnas.97.21.11403.

Kimmel, C.B., Ballard, W.W., Kimmel, S.R., Ullmann, B., Schilling, T.F., 1995. Stages of embryonic development of the zebrafish. Dev. Dyn. 203, 253–310. https://doi.org/10.1002/aja.1002030302.

Klein, J.C., Agarwal, V., Inoue, F., Keith, A., Martin, B., Kircher, M., Ahituv, N., Shendure, J., 2020. A systematic evaluation of the design and context dependencies of massively parallel reporter assays. Nat. Methods 17, 1083–1091. https://doi.org/10.1038/s41592-020-0965-y.

Kwasnieski, J.C., Fiore, C., Chaudhari, H.G., Cohen, B.A., 2014. High-throughput functional testing of ENCODE segmentation predictions. Genome Res. 24, 1595–1602. https://doi.org/10.1101/gr.173518.114.

LaBelle, J., Ramos-Martinez, A., Shen, K., Motta-Mena, L.B., Gardner, K.H., Materna, S. C., Woo, S., 2021. TAEL 2.0: an improved optogenetic expression system for zebrafish. Zebrafish 18, 20–28. https://doi.org/10.1089/zeb.2020.1951.

Lalonde, R.L., Wells, H.H., Kemmler, C.L., Nieuwenhuize, S., Lerma, R., Burger, A., Mosimann, C., 2024. pIGLET: safe harbor landing sites for reproducible and efficient

transgenesis in zebrafish. Sci. Adv. 10, eadn6603. https://doi.org/10.1126/sciadv.adn6603.
Lawson, N.D., Weinstein, B.M., 2002. In vivo imaging of Embryonic vascular development using transgenic zebrafish. Dev. Biol. 248, 307–318. https://doi.org/10.1006/dbio.2002.0711.
Lee, T.I., Young, R.A., 2013. Transcriptional regulation and its misregulation in disease. Cell 152, 1237–1251. https://doi.org/10.1016/j.cell.2013.02.014.
Ligunas, G.D., Materna, S.C., 2026. Quantification of eef1a1l1 transcript in early zebrafish development. MicroPublication Biol. https://doi.org/10.17912/micropub.biology.001944.
Manoli, M., Driever, W., 2012. Fluorescence-activated cell sorting (FACS) of fluorescently tagged cells from zebrafish larvae for RNA isolation. Cold Spring Harb. Protoc. https://doi.org/10.1101/pdb.prot069633, 2012.
McCurley, A.T., Callard, G.V., 2008. Characterization of housekeeping genes in zebrafish: male-female differences and effects of tissue type, developmental stage and chemical treatment. BMC Mol. Biol. 9 (1), 102. https://doi.org/10.1186/1471-2199-9-102.
Mosimann, C., Kaufman, C.K., Li, P., Pugach, E.K., Tamplin, O.J., Zon, L.I., 2011. Ubiquitous transgene expression and Cre-based recombination driven by the *ubiquitin* promoter in zebrafish. Development 138, 169–177. https://doi.org/10.1242/dev.059345.
Motta-Mena, L.B., Reade, A., Mallory, M.J., Glantz, S., Weiner, O.D., Lynch, K.W., Gardner, K.H., 2014. An optogenetic gene expression system with rapid activation and deactivation kinetics. Nat. Chem. Biol. 10, 196–202. https://doi.org/10.1038/nchembio.1430.
Nam, J., Dong, P., Tarpine, R., Istrail, S., Davidson, E.H., 2010. Functional *cis* -regulatory genomics for systems biology. Proc. Natl. Acad. Sci. 107, 3930–3935. https://doi.org/10.1073/pnas.1000147107.
Pennacchio, L.A., Bickmore, W., Dean, A., Nobrega, M.A., Bejerano, G., 2013. Enhancers: five essential questions. Nat. Rev. Genet. 14, 288–295. https://doi.org/10.1038/nrg3458.
Peter, I.S., Davidson, E.H., 2015. Genomic Control Process: Development and Evolution, 1. Aufl. Academic Press, Elsevier, Amsterdam Heidelberg.
Rabani, M., Pieper, L., Chew, G.-L., Schier, A.F., 2017. A massively parallel reporter assay of 3′ UTR sequences identifies in vivo rules for mRNA degradation. Mol. Cells 68, 1083–1094.e5. https://doi.org/10.1016/j.molcel.2017.11.014.
Reimão-Pinto, M.M., Castillo-Hair, S.M., Seelig, G., Schier, A.F., 2025. The regulatory landscape of 5′ UTRs in translational control during zebrafish embryogenesis. Dev. Cell 60, 1498–1515.e8. https://doi.org/10.1016/j.devcel.2024.12.038.
Ryan, G.E., Farley, E.K., 2020. Functional genomic approaches to elucidate the role of enhancers during development. WIREs Syst. Biol. Med. 12. https://doi.org/10.1002/wsbm.1467.
Sacilotto, N., Monteiro, R., Fritzsche, M., Becker, P.W., Sanchez-del-Campo, L., Liu, K., Pinheiro, P., Ratnayaka, I., Davies, B., Goding, C.R., Patient, R., Bou-Gharios, G., De Val, S., 2013. Analysis of *Dll4* regulation reveals a combinatorial role for Sox and Notch in arterial development. Proc. Natl. Acad. Sci. 110, 11893–11898. https://doi.org/10.1073/pnas.1300805110.
Scott, E.K., 2009. The cellular architecture of the larval zebrafish tectum, as revealed by Gal4 enhancer trap lines. Front. Neural Circ. 3. https://doi.org/10.3389/neuro.04.013.2009.
Singh, G., Mullany, S., Moorthy, S.D., Zhang, R., Mehdi, T., Tian, R., Duncan, A.G., Moses, A.M., Mitchell, J.A., 2021. A flexible repertoire of transcription factor binding sites and a diversity threshold determines enhancer activity in embryonic stem cells. Genome Res. 31, 564–575. https://doi.org/10.1101/gr.272468.120.
Sur, A., Wang, Y., Capar, P., Margolin, G., Prochaska, M.K., Farrell, J.A., 2023. Single-cell analysis of shared signatures and transcriptional diversity during zebrafish development. Dev. Cell S1534580723005774. https://doi.org/10.1016/j.devcel.2023.11.001.
Suster, M.L., Kikuta, H., Urasaki, A., Asakawa, K., Kawakami, K., 2009. Transgenesis in zebrafish with the Tol2 Transposon system. In: Cartwright, E.J. (Ed.), Transgenesis Techniques, Methods in Molecular Biology. Humana Press, Totowa, NJ, pp. 41–63. https://doi.org/10.1007/978-1-60327-019-9_3.
Taylor, S.C., Nadeau, K., Abbasi, M., Lachance, C., Nguyen, M., Fenrich, J., 2019. The ultimate qPCR experiment: producing publication quality, reproducible data the first time. Trends Biotechnol. 37, 761–774. https://doi.org/10.1016/j.tibtech.2018.12.002.
The ENCODE Project Consortium, 2012. An integrated encyclopedia of DNA elements in the human genome. Nature 489, 57–74. https://doi.org/10.1038/nature11247.
Untergasser, A., Cutcutache, I., Koressaar, T., Ye, J., Faircloth, B.C., Remm, M., Rozen, S. G., 2012. Primer3–new capabilities and interfaces. Nucleic Acids Res. 40, e115. https://doi.org/10.1093/nar/gks596.
Wagner, D.E., Weinreb, C., Collins, Z.M., Briggs, J.A., Megason, S.G., Klein, A.M., 2018. Single-cell mapping of gene expression landscapes and lineage in the zebrafish embryo. Science 360, 981–987. https://doi.org/10.1126/science.aar4362.
Wan, Y., El Kholtei, J., Jenie, I., Colomer-Rosell, M., Liu, J., Zhang, Q., Navajas Acedo, J., Du, L.Y., Codina-Tobias, M., Wang, M., Zheng, W., Lin, E., Chuang, T.-H., Mayseless, O., Sawh, A., Mango, S.E., Yu, G., Bintu, B., Schier, A.F., 2026. Whole-embryo spatial transcriptomics at subcellular resolution from gastrulation to organogenesis. Science 391, eadt3439. https://doi.org/10.1126/science.adt3439.
Wang, J., Dai, X., Berry, L.D., Cogan, J.D., Liu, Q., Shyr, Y., 2019. HACER: an atlas of human active enhancers to interpret regulatory variants. Nucleic Acids Res. 47, D106–D112. https://doi.org/10.1093/nar/gky864.
Ward, L.D., Kellis, M., 2012. Evidence of abundant purifying selection in humans for recently acquired regulatory functions. Science 337, 1675–1678. https://doi.org/10.1126/science.1225057.
Westerfield, M., 2007. The Zebrafish Book. A Guide for the Laboratory Use of Zebrafish (Danio rerio), fifth ed. University of Oregon Press, Eugene. Oregon.
Williams, R.M., Candido-Ferreira, I., Repapi, E., Gavriouchkina, D., Senanayake, U., Ling, I.T.C., Telenius, J., Taylor, S., Hughes, J., Sauka-Spengler, T., 2019. Reconstruction of the global neural crest gene regulatory network in vivo. Dev. Cell 51, 255–276.e7. https://doi.org/10.1016/j.devcel.2019.10.003.
Williams, R.M., Sauka-Spengler, T., 2021. Rapid and efficient enhancer cloning and in vivo screening using the developing chick embryo. STAR Protoc. 2, 100507. https://doi.org/10.1016/j.xpro.2021.100507.
Wong, M.L., Medrano, J.F., 2005. Real-time PCR for mRNA quantitation. Biotechniques 39, 75–85. https://doi.org/10.2144/05391RV01.